Available online at www.sciencedirect.com
ScienceDirect
Journal of Sound and Vibration 301 (2007) 28–42
JOURNAL OF SOUND AND VIBRATION
www.elsevier.com/locate/jsvi

Propagation of the initial transient noise from an impacted plate

Annie Ross*, Germain Ostiguy

Department of Mechanical Engineering, École Polytechnique de Montréal, CP 6079 succ. Centre-ville, Montréal (Qué), Canada H3C 3A7

Received 22 March 2004; received in revised form 7 August 2006; accepted 4 September 2006
Available online 28 November 2006

Abstract

The near field initial transient noise of an impacted plate is studied, and the means of propagation of this noise is examined. Impacts are performed by a rigid spherical object at the center of a thin rectangular plate. Two different impact energy levels are produced. Acoustic pressure time-histories are obtained analytically and experimentally at four different locations near the impact point. An analytical model is produced, based on the classical theory of thin plate, Rayleigh's surface integral, and modified Hertzian force. The results are in good agreement with the experiments. They show that on the impact axis (normal to the plate), the initial transient noise is similar to the acceleration noise of a piston subjected to the same force signal, and that the waveform shape varies with the impact energy level. Off-axis initial transient waveforms are examined through the analytical solution, and two different partial solutions. Results show that the initial transient noise of an impacted plate is partially structure-borne. Continuity with the initial bending wave causes the initial transient noise to be dispersive. The effects of dispersion are negligible in the vicinity of the impact axis, but become considerable at large observation angles.

1. Introduction

The transverse dynamic response of impacted structures includes a forced elastic response during the contact and a free vibration resulting from the impulse. Ringing noise is a long transient, mainly caused by the free transverse vibration of the entire structure after the impact. It forms a "pseudo-steady-state radiation from natural modes" of the structure [1]. A much shorter transient noise, in the order of the ms, is caused by the sudden, forced deformation of the structure in the contact area.

During a collision between rigid bodies such as steel spheres, or a sphere and a massive plane, the short transient is referred to as "rigid-body radiation" or "acceleration noise" [1,2]. Ringing in the rigid bodies may be neglected, and the acceleration noise itself may be identified [3]. When an impact occurs on a large, flexible structure, however, only part of the structure is initially deformed during the contact. This initial elastic deformation spreads through the structure by means of various transient waves, including a bending wave. The resulting acoustic radiation is a short transient referred to as the "initial pressure pulse" or the "initial transient acoustic wave" [1,4].

*Corresponding author. Fax: +1 514 340 41 76.
E-mail address: Annie.Ross@polymtl.ca (A. Ross).

0022-460X/$ - see front matter © 2006 Elsevier Ltd. All rights reserved.
doi:10.1016/j.jsv.2006.09.016

Akay and Latcha have observed the sound pressure waveform of an impacted plate [5]. Their experiments clearly showed a distinct initial pulse and a "silent" time period, before the ringing noise is detected on the impact axis (normal to the plate, passing through the impact point). Off-axis measurements also showed that a time-overlap occurs between the initial pulse and the ringing noise (also shown by Heitkämper [6]). The time overlap increases with the observation angle, to the point where the initial pulse becomes indiscernible.

The current literature does not entirely cover the propagation mechanism of the initial transient noise of an impacted plate. Wåhlin, Gren and Molin have performed double-pulse interferograms to show that initial sound wave fronts propagate at an angle from the plate, and that this propagation angle is frequency dependent [4]. Analytic work by Heitkämper also resulted in oblique wave fronts [6]. As suggested by Wåhlin et al., the initial pressure pulse is partly propagated via the supersonic components of the initial flexural wave in the plate, which "act as a series of traveling acoustic sources, generating trace matched acoustic waves". Based on this assumption, and knowing that bending waves are dispersive, it is expected that high-frequency components in the initial transient noise will reach off-axis observation points faster than low frequency components. The initial transient acoustic wave would therefore be dispersive in off-axis directions, resulting in a shifting waveform. However, the sound pressure waveforms shown in the literature do not adequately support this assumption. Published data either do not display the signs of a dispersed wave, due to the locations of the observation points, or are misinterpreted due to overlapping ringing noise.

The purpose of this paper is to demonstrate that the initial transient noise of a flexible plate is partly structure borne, and that it can be modeled by considering the dispersive flexural waves within the plate. Acoustic pressure measurements, as well as a classic analytical model are used to provide reliable data on the near field initial transient noise. A partial analytical model is developed on the basis of a partly dispersive sound wave, and resulting waveforms are compared with actual data.

2. Transient radiation from a rectangular plate

With reference to Fig. 1, let us consider a rectangular metal plate of dimensions $a \times b$, thickness h and mass m. Three coordinate systems are placed on this plate. Cartesian coordinates X, Y, Z originate at one corner of the plate, with X and Y parallel to the sides of the plate. Cylindrical coordinates R, ψ, z, and polar coordinates r, ϕ, θ both originate at the center of the plate. Suppose that a metallic sphere of radius $\mathscr{R}$ strikes the center of the plate with a velocity v_o.

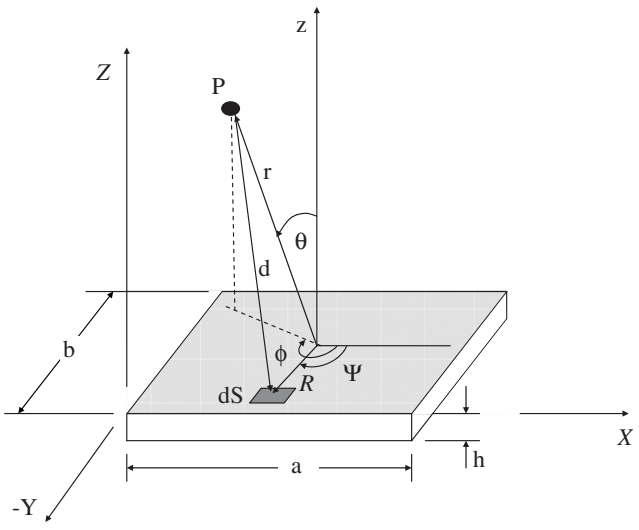

Fig. 1. Rectangular plate and coordinate systems.

2.1. Impact force

According to the Hertz theory of contact, the impact force of a sphere onto a massive plane is given by [7]

$$F(t) = F \sin\left(\frac{\pi t}{\tau}\right). \tag{1}$$

Eq. (1) is valid for the duration of the Hertzian contact $0 \leqslant t \leqslant \tau$. The magnitude F depends on the size of the sphere, on the impact velocity, as well as on the mechanical and physical properties of the sphere and the massive plane. A better approximation was shown to be applicable for flexible planes such as thin plates [6]:

$$F(t) \approx F\left\{\frac{1.1}{1+\Lambda+2\Lambda^2}\sin(0.97T)^{1.5}\exp\left[-(0.4T)^4\right] + \left(\frac{1+2/\Lambda}{1+\Lambda}\right)\left(\frac{T}{T+1/\Lambda}\right)^{1.5}\exp\left(\frac{-T}{\Lambda}\right)\right\}, \tag{2}$$

where $T = \pi t/\tau$ is the non-dimensional time, F is the Hertzian contact force. Parameter Λ is related to the impact energy and the flexibility of the plate. It is defined as

$$\Lambda = 1.15\left(\frac{\mathscr{R}}{h}\right)^2\left(\frac{v_o}{C_L}\right)^{0.2}\left(\frac{\rho_b}{\rho_p}\right)^{0.6}\left(\frac{E'_b}{E'_b+E'_p}\right)^{0.4}, \tag{3}$$

and

$$E' = \frac{E}{1-v^2}.$$

Variables ρ, E and v are, respectively, the mass density, Young's modulus and Poisson's ratio of the plate (subscript p) or the sphere (subscript b). C_L is the speed of longitudinal waves within the plate: it is taken as 5160 m/s in aluminum, and 5060 m/s in steel [8]. When the sphere is light and the impact velocity is weak, the impact energy is low and the value of Λ is small. In addition, if the plate is heavy and rigid, it will not yield much, and Λ will be even smaller. Low energy impacts on a massive plane will produce $\Lambda \to 0$. In Eq. (2), it should be noted that when $\Lambda \ll 1$, the first term is dominant, whereas the second term becomes dominant when $\Lambda \gg 1$. Therefore, the time signal of the contact force depends largely on the value of Λ. In addition, for large values of Λ, the duration of the flexible contact (τ') can be much longer than the duration of the Hertzian contact (τ).

2.2. Transverse acceleration of the plate

The classical theory of plates gives the transverse displacement $u(X, Y, t)$ of plate element $\mathrm{d}S(X, Y)$ as a summation over modes j and k. For a plate that is simply supported along all four edges (s–s–s–s), transverse displacement is given by [7]

$$u(X,Y,t) = \frac{-4}{m}\sum_j\sum_k \frac{\sin(j\pi/2)\sin(k\pi/2)\sin(j\pi X/a)\sin(k\pi Y/b)}{\omega_{jk}} \times\left[F(t) * \sin(\omega_{jk}t)\right], \tag{4}$$

where $A*B$ is the symbol for convolution. When impacts occur at the center of the plate, only odd numbered modes are excited (j and $k = 1,3,5,\ldots$). The symmetry of the transverse displacements can be shown when a change of coordinates is applied:

$$u(R,\psi,t) = \frac{-4}{m}\sum_j\sum_k \frac{(-1)^{\frac{j-1}{2}}(-1)^{\frac{k-1}{2}}}{\omega_{jk}}\sin\left(\frac{j\pi}{2}+\frac{j\pi R\cos\psi}{a}\right) \sin\left(\frac{k\pi}{2}+\frac{k\pi R\sin\psi}{b}\right)\left[F(t) * \sin(\omega_{jk}t)\right]. \tag{5}$$

A numerical evaluation of the above equation was performed in a low energy impact configuration on a large thin plate (described in Section 3.1). Over 30 equally spaced radii $R<a/2$ and 20 different angles ψ from 0 to 2π were considered. Time was varied between τ (the duration of contact) and 3τ (the time required by the initial bending wave to reach the plate supports). A summation over 400 odd modes ($i, k \leqslant 39$) clearly showed that the variations of u with respect to ψ are at least 2 orders of magnitude lower than the maximum deformations of the plate. The initial propagation of the bending wave is therefore considered symmetrical about the z-axis

$$\frac{\partial u(R,\psi,t)}{\partial \psi} \approx 0. \tag{6}$$

The transverse acceleration of the plate is given by $\partial^2 u/\partial t^2$. Because $u(R, \psi, t)$ is no longer a function of the angular position ψ, this angle may be selected arbitrarily. Any multiple of $\pi/2$ is a wise choice, because it reduces the number of computational operations. By selecting $\psi = 0$, the transverse acceleration of the plate becomes

$$\ddot{u}(R,t) = \frac{-4}{m}\sum_j \sum_k (-1)^{\frac{j-1}{2}} \sin\left[j\pi\left(\frac{1}{2}+\frac{R}{a}\right)\right] \times \left[\frac{\mathrm{d}F}{\mathrm{d}t} * \cos(\omega_{jk} t)\right]. \tag{7}$$

The initial transient acceleration of the plate is also symmetrical about the z-axis (also known as the impact axis).

2.3. Radiated acoustic pressure

The transverse displacement of an impacted plate is often very small, compared to the thickness of the plate. In that case, one may consider the plate as a plane source in an infinite baffle. When reflection and diffraction of sound at the boundaries of the plate are ignored, the sound pressure radiated at a point P in the ambient medium can be obtained from Rayleigh's surface integral [5]:

$$p(r,\phi,\theta,t) = \frac{\rho}{2\pi}\iint \ddot{u}\left(R,\psi,t-\frac{d}{c}\right)\frac{\mathrm{d}S}{\mathrm{d}}, \tag{8}$$

where ρ is the density of the medium (air) and c the acoustic wave speed in the medium. $\ddot{u}\left(R,\psi,t-d/c\right)$ is the transverse acceleration of plate element $\mathrm{d}S$, calculated from Eq. (7), and applied with the appropriate time delay d/c. Plate element $\mathrm{d}S = \mathrm{d}R R\,\mathrm{d}\psi$ is located at a position R, ψ on the plate, from the impact point. Point P is located at position r, ϕ, θ; it represents the position where the acoustic pressure is to be obtained. For any position P along the plane $\phi = 0$, distance d is calculated from plate element $\mathrm{d}S$ to point P from

$$d = \sqrt{(r\sin\theta - R\cos\psi)^2 + (R\sin\psi)^2 + (r\cos\theta)^2}. \tag{9}$$

Because the transverse acceleration is axisymmetric, we may write

$$p(r,\phi,t) = \frac{\rho}{2\pi}\int_R \int_\psi \ddot{u}\left(R, t-\frac{d}{c}\right)\frac{\mathrm{d}R R\,\mathrm{d}\psi}{d}. \tag{10}$$

Although d is a function of ψ, the initial pressure field is considered symmetrical about the z-axis, because the transverse acceleration is integrated over the range $0 \leqslant \psi \leqslant 2\pi$. Experiments discussed in Section 3.1 confirm this observation. The acoustic pressure field is therefore written as

$$p(r,\theta,t) = \frac{-2\rho}{\pi m}\int_R \int_\psi \sum_j \sum_k (-1)^{\frac{j-1}{2}} \sin\left[j\pi\left(\frac{1}{2}+\frac{R}{a}\right)\right] \times \left[\frac{\mathrm{d}F}{\mathrm{d}t}(t-d/c) * \cos\left(\omega_{jk}(t-d/c)\right)\right]\frac{\mathrm{d}R R\,\mathrm{d}\psi}{d}, \tag{11}$$

where the force $F(t)$ is zero at all times, except during the contact period $0 \leqslant t \leqslant \tau'$. In view of the fact that the initial transient noise is symmetrical about the impact axis, the following calculations were performed along a single plane, normal to the plate ($\phi = \text{constant}$).

3. Calculations based on the analytical equations

It was mentioned in Section 2.1 that the shape of the force signal varies with the value of Λ. One may thus expect the acoustic pressure time signal to be different, depending on Λ. For this reason, calculations were performed on the basis of Eqs. (2), (3) and (11). The mechanical s–s–s–s rectangular plate was subjected to a transverse impact at its center. Two configurations were tested. In configuration A, low impacts ($\Lambda < 1$) were studied, and results were compared with experimental measurements. Relatively, high energy impacts ($\Lambda > 1$) in configuration B were compared with results given in the literature. The impact energy level refers to the amount of energy transferred to the plate during the impact. Low energy impacts require a light hammer and a low contact speed. A thicker plate generates a higher impact force, but it also is less compliant, and it causes an even lower impact energy level.

3.1. Configuration A: low energy impact

In configuration A, a ball-ended hammer was striking the center of a 0.6 m × 0.9 m × 4.8 mm aluminum plate. The steel ball was 6.4 mm in diameter, and the hammer weighed 26.8 g. The velocity of the hammer was evaluated at 0.23 m/s, using the data from an accelerometer placed on top of the hammer. According to Eq. (3), the value of parameter Λ was 0.11. Results calculated from configuration A were compared with experimental measurements on a similar set up.

The initial acoustic pressure in Fig. 2 (shown as a solid line) was calculated on the impact axis, in the near field of the impact point ($r = 50$ mm and $0 = 0^\circ$). Also shown as a dashed line is the calculated impact force. It should be noted that the force signal was applied with a time delay that corresponds to the distance traveled by the acoustic wave (50 mm) at a speed of 343 m/s. To allow for an easier comparison, the force's amplitude was reduced by a factor of -4.7 to match the amplitude of the pressure signal. Because the calculations were performed on the impacted side of the plate, the initial acoustic pressure peak is negative. (It is positive on the other side of the plate.) The shape of this initial peak is nearly identical to that of the force signal, as expected from the literature [5]. Its duration is approximately 0.14 ms. At the end of contact, an oscillation develops gradually: it is the ringing noise. In this impact configuration and at this position in the acoustic field, the

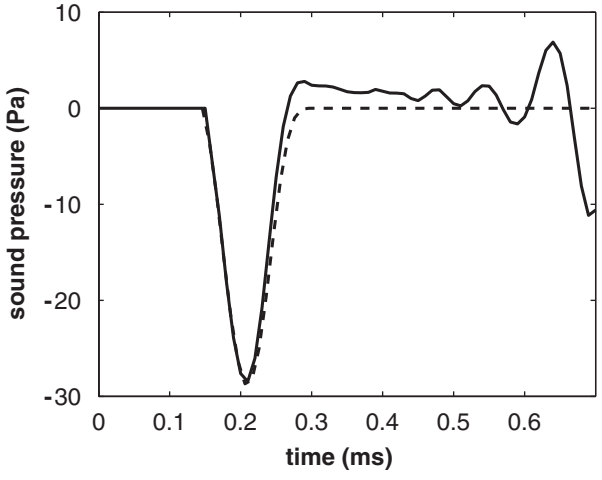

Fig. 2. Initial transient acoustic pressure due to a low velocity impact at a distance of 50 mm from the plate, and observation angle $\theta = 0^\circ$: — is the pressure calculated using Eqs. (2), (3) and (11); - - - is the impact force function with time delay and reduced amplitude.

overlap between the initial transient and the ringing noise is practically inexistent. Both the initial transient noise and the impact force in Fig. 2 can be approximated with a sinusoid, rather than an exponentially decreasing curve. Clearly, the second term of the force function (Eq. (2)) is negligible in this case.

In Fig. 3, the initial transient acoustic pressure in the near field of the impact point was both calculated and measured at different near field positions. Both experimental measurements and calculations were carried out over a plane grid located 50 mm parallel to the surface of the impacted plate. The four observation points (P) were taken at $\theta = 23^\circ$, 52°, 64°, and 71° from the z-axis from frame (a) to frame (d), respectively. The solid lines represent the calculated acoustic pressure, and discrete points are the experimental data points. (Experiments were performed in an anechoic environment. Data was sampled at 32 kHz and averaged over 30 samples. Analog trigger and pre-trigger scans were used to capture the entire initial acoustic signal.) As shown in Fig. 3, the initial peaks of the calculated and experimental results are in good agreement These peaks correspond to the initial transient acoustic pressure. All observation points were located on the same side of the plate where the impact occurred, resulting in a rarefactive initial pressure pulse along the impact axis. The signal that follows the initial peaks is the ringing noise. In the experimental data, the acoustic pressure that precedes the main peaks is attributable to a low level residual ringing noise from the previous blow on the plate (the plate was impacted at a rate of 27 Hz). Small differences may occur in the ringing noise due to

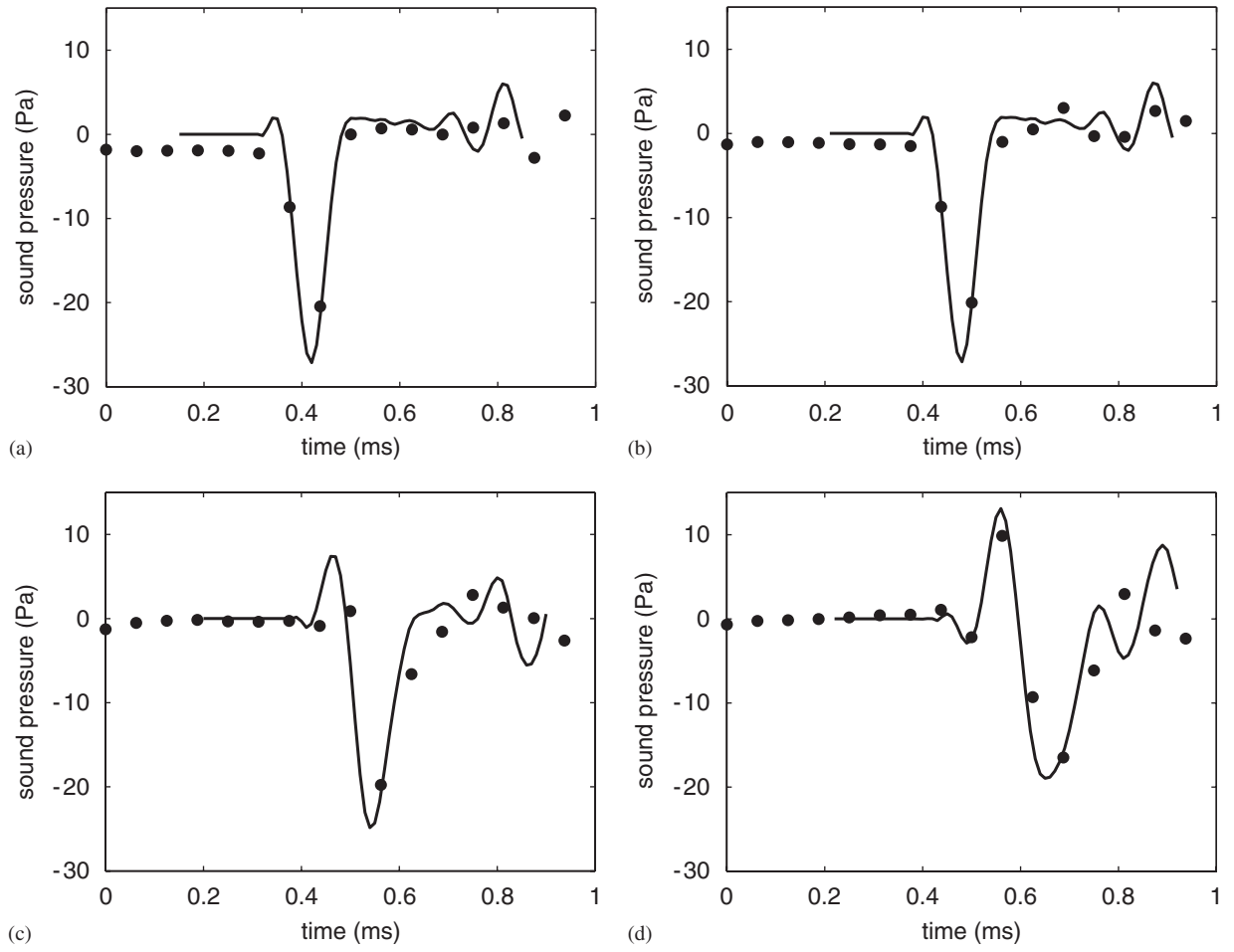

Fig. 3. Initial transient acoustic pressure due to a low velocity impact at a distance of 50 mm from the plate: — is calculated using Eqs. (2), (3) and (11); ● is measured on an experimental set up. Observation angle θ is 23° in frame (a), 52° in frame (b), 64° in frame (c), and 71° in frame (d).

possible imperfections in the experimental impact and support conditions. In addition, the calculations do not account for the acoustic energy radiated from the edges of the plate. Changes in the initial pressure signal can be observed as the survey point (P) is moved away from the impact axis, from frames (a) to (d). A very short time delay (0.04 ms between frames (a) and (d)) occurs at the beginning of the time signal when the survey point is farther from the impact point. Acoustic airwave propagation cannot account for such a short time delay: it would take an acoustic airwave approximately 0.3 ms to travel the distance separating these two points. Meanwhile, a positive initial peak develops ahead of the negative peak discussed earlier and shown in Fig. 2. Other initial peaks also form when the observation angle is large. These observations are discussed in Section 4. The ringing noise still develops gradually, but the overlap with the initial transient noise becomes more significant.

Experimental measurements were also used to confirm the symmetry of the initial pressure field, predicted by the theory in Section 2.3. Measurement points were located in an evenly spaced 8×8 lattice on the measurement plane (described above). A 0.4 ms flat-top window was used on the initial transient noise. Initial transient sound pressure levels (SPL) were calculated over the $210 \times 210\,\text{mm}^2$ measurement area, centered about the impact axis. In Fig. 4, are shown concentric, relatively circular curves [9]. Obviously, experimental discrepancies and time-windowing, may have caused the slightly irregular circular shape of the contours. Nonetheless, the results shown in Fig. 4 support the assumption that the initial transient noise is axisymmetric, even when the impacted plate is not circular.

3.2. Configuration B: high energy impact

In configuration B, a steel sphere of radius 12.7 mm hits a $0.6\,\text{m} \times 0.9\,\text{m} \times 2\,\text{mm}$ steel plate, with an impact velocity of 1 m/s. Parameter Λ has a value of 6.36. This impact configuration is similar to that used by Heitkämper [6]. It is considered a high energy impact, due to the higher contact speed, the mass of the sphere and the thinness of the plate. Examination of configuration B serves two purposes: the first is to evaluate the analytical model, and the second is to serve as a comparison for configuration A.

In Fig. 5 is shown the initial acoustic pressure (solid line) calculated at the same four positions used to generate the results of Fig. 3 (i.e., at 50 mm from the surface of the plate, and at observation angles $\theta = 23^\circ$, 52°, 64°, and 71° from the z-axis. As in Fig. 2, the dashed line represents the impact force, applied with the proper acoustic wave propagation delay for the given positions. Again, for comparison purposes, the amplitude of the force was reduced to match that of the acoustic pressure signal. The shape of the acoustic pressure signals obtained in frames (a), $\theta = 23^\circ$, and (c), $\theta = 64^\circ$, are comparable to Heitkämper's results at similar positions [6]. Along the impact axis (frame(a)), the initial transient noise is characterized by its rapid

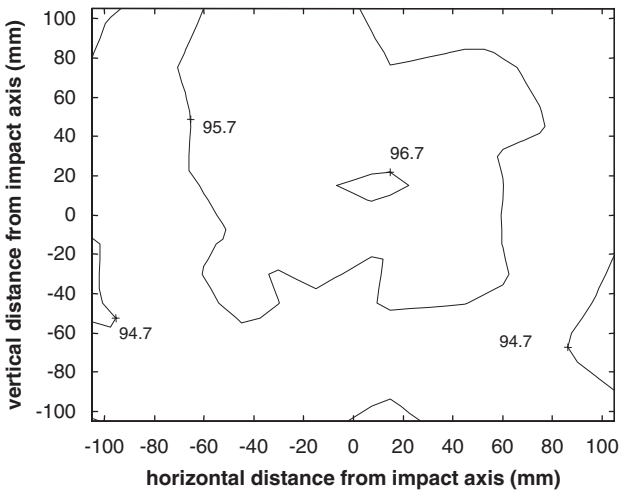

Fig. 4. Sound pressure level contours of initial transient noise measured at 50 mm from the plate, showing symmetry about z-axis [9].

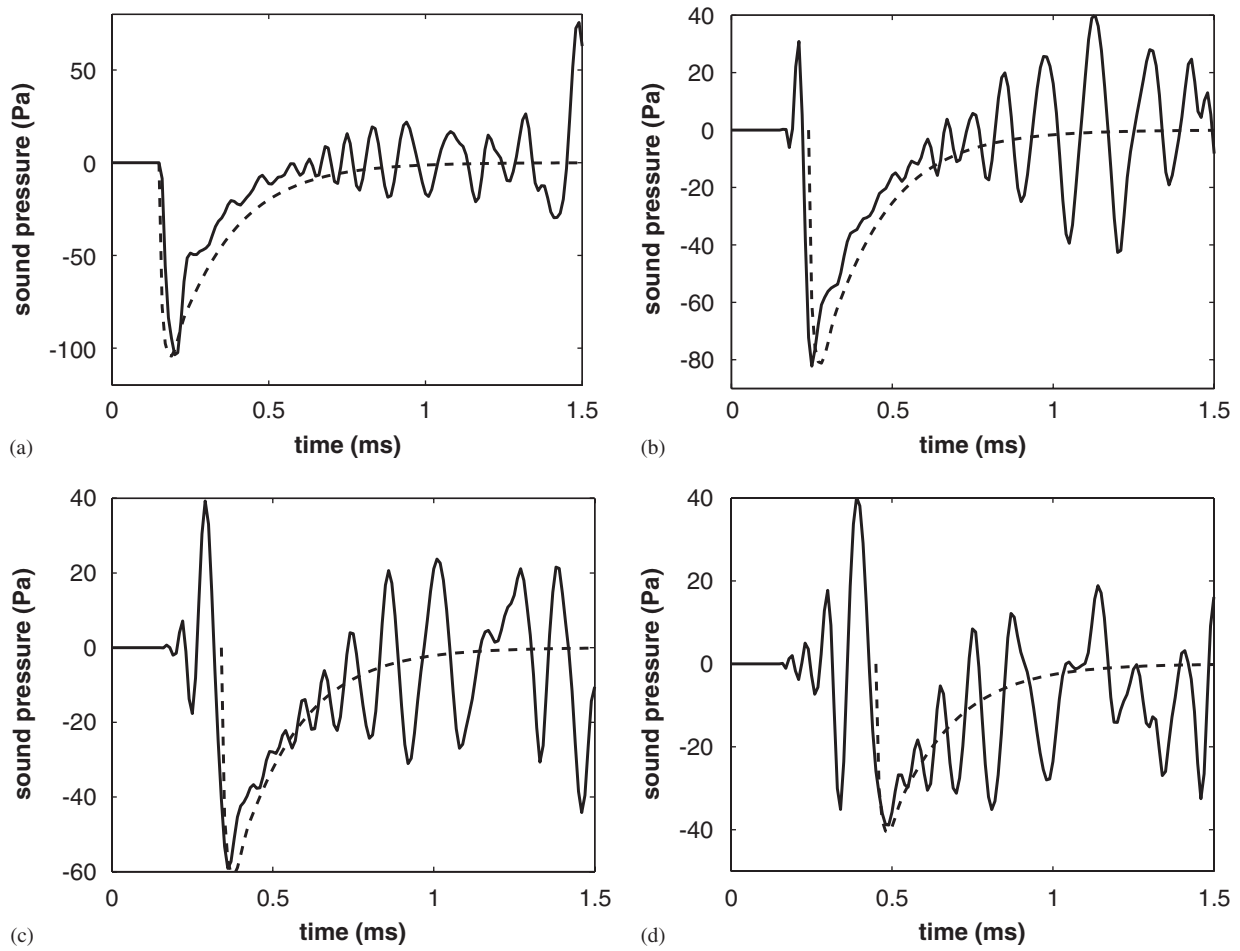

Fig. 5. Initial transient acoustic pressure due to a high velocity impact at a distance of 50 mm from the plate: — is calculated using Eqs. (2), (3) and (11); - - - is the impact force function with time delay and amplitude decay. Observation angle θ is 23° in frame (a), 52° in frame (b), 64° in frame (c), and 71° in frame (d).

rise and slower exponential decrease. As in configuration A, the initial transient noise closely follows the shape of the impact force. From the slow exponential decrease, it appears that the second term of Eq. (2) is much more significant in this high-energy configuration than it is in configuration A. Again, ringing noise is seen as an increasing oscillation. The time overlap between the initial transient and the ringing noise is due to the much longer duration of the initial transient noise (here, the contact duration is almost 6 times longer than that in configuration A).

When the survey point (P) is moved away from the impact axis, from frame (a) to frame (d), changes in the initial pressure signal are similar to those observed in configuration A. The time delay between the various positions is, again, extremely short. Part of the acoustic pressure signal continues to follow the impact force (dashed lines), but is preceded by large pressure oscillations. These oscillations are considerable, when compared to what the ringing noise is expected to be in such a short time after the impact. The size and the number of these initial peaks increase with the observation angle.

Propagation of the initial transient noise is discussed in Section 4. However, one conclusion can be stated at this time: along the impact axis, the initial transient noise can be determined, and the waveform shape is similar to that of the impact force. The acoustic waveform varies according to the impact force for different impact energy levels.

4. Propagation of the initial transient noise

One important aspect of this work is to sort out the contributions of the initial transient wave and ringing noise to the time signal, when a flexible structure is impacted. (Note that the ringing noise results from the free vibration modes of the plate and does not include the initial flexural wave traveling outward from the impacted area until it reaches the edges of the plate.) It is generally accepted that the time overlap between the initial pulse and ringing increases with the observation angle. However, the nature of acoustic pressure oscillations at the very beginning of the signal when $\theta >> 0$ is not explained in the literature. It has been referred to as the ringing noise (e.g. Ref. [6]). The following discussion specifically aims at determining whether these initial acoustic pressure oscillations belong to the initial transient noise or to the ringing noise. Two hypotheses are examined, as to how the initial transient noise propagates.

4.1. First hypothesis: piston-like behavior

In this hypothesis, the entire initial noise is a pure airwave, as would be the case for a rigidly baffled piston. In this case, propagation in air would cause a time delay and amplitude decay in the signal as the observation point P is moved away from the impact point. However, the shape of the initial noise would remain unchanged. The initial oscillations would then belong to the ringing noise. Fig. 6 illustrates such propagation.

Transient acoustic pressure signals were calculated using Eq. (10) for various locations in the acoustic field of the impacted plate (Fig. 6a), and a baffled, 30 mm-radius piston (Figs. 6b and c). All calculation points were located at 50 mm from the plate or baffle, in distance increments of 20 mm from the impact axis or piston axis. Heavy lines highlight results at 0 mm (full line) and 100 mm (dashed) from the axis. A low energy impact was considered on the plate, as in Section 3.1. In Fig. 6b, the piston was subjected to the same force history as was applied in the case of the impacted plate, and the acceleration was calculated by using

$$\ddot{u}(t) = \frac{\mathrm{d}^2}{\mathrm{d}t^2}\left[\frac{1}{m\omega_n}\sin(\omega_n t) * F(t)\right]. \tag{12}$$

The natural half-period (π/ω_n), chosen as 2 ms, is considerably longer than the duration of the force. (A great number of modes in the plate have even lower natural frequencies.) Hereafter, this case is referred to as the "forced piston". In Fig. 6c, the piston was subjected to the same acceleration history as was observed at the impact point on the plate. This case is referred to as the "accelerated piston". No reflection or diffraction was considered in either system. Observations from Fig. 6 are discussed below.

First, the acceleration noise of the "forced piston" (Fig. 6b) and the "accelerated piston" (Fig. 6c) are quite different. On the piston axis (0 mm), the pressure signal of the "accelerated piston has the same "reversed N" shape as the imposed acceleration. Such a relationship is expected from Eq. (10). The U-shaped pressure signal of the "forced piston", however, clearly indicates that the acceleration history of the "forced piston" is different. Therefore, the acceleration of the piston is not the same as that of the plate when subjected to the same force.

Second, when calculations are performed at a distance from the piston axis, both time delay and amplitude decay can be observed in Figs. 6b and c. As expected from present knowledge, the pressure amplitude decreases more rapidly with respect to propagation angle than it would if it were a spherical wave. For instance, the acceleration noise pressure at 100 mm from the piston axis ($r = 111$ mm, and $\theta = 63^\circ$) is 68% lower than it is at 0 mm (r = 50 mm, and $\theta = 0^\circ$) for the "forced piston" and 82% lower for the "accelerated piston". In a spherical wave, the attenuation would be 55% for the same distance. Aside from the expected changes described above, no major changes can be seen in the shape of the time signals with respect to the position.

Third, the acoustic pressure time signal is similar on the impact axis of the plate and on the axis of the "forced piston" (0 mm). Although it was stated above that the acceleration of the plate and the piston's acceleration are not the same, the "U" shape and duration of both signals are similar to that of the force signal. Thus, the piston-like initial transient noise of the plate in the impact axis is not produced by a piston-like motion.

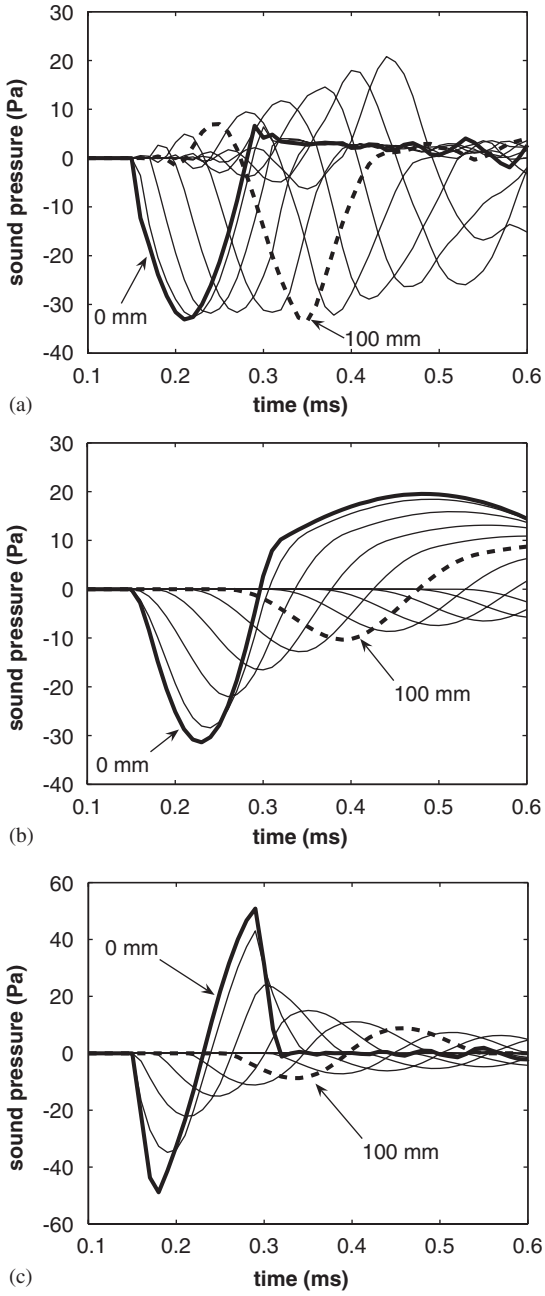

Fig. 6. Calculated transient acoustic pressure at 50 mm from plate or baffle, in distance increments of 20 mm from the impact axis: (a) low energy impact on plate; (b) baffled rigid piston imposed with same force as plate; (c) baffled rigid piston imposed with same acceleration as impact point on plate.

Finally, the shapes of the time signals observed at various distances from the impact axis of the plate differ from point to point (Fig. 6a), in the way that is not piston-like. For one, the sound attenuation with the distance is much less than that observed on the piston. Moreover, the initial single negative peak (at 0 mm) develops into an N-shaped signal as a positive peak develops when distance is increased (clearly visible at 100 mm). This positive peak starts appearing at times when ringing has not yet developed. (Ringing can be recognized as the higher frequency, very low amplitude oscillations at the end of the initial pressure peak on the 0 mm signal.) Actually, it can be seen that ringing pressure oscillations remain very low until time 0.4 ms,

whereas the positive peak discussed starts appearing as early as 0.2 ms. Other similar peaks appear as the distance increases, in a pattern similar to that of a dispersive wave.

In summary, the initial transient noise of the plate is different to that resulting from a piston subjected to either the same force or acceleration as the impact point of the plate. Although the transient waveforms on the impact axis and "forced piston" axis (0 mm) are close, this seems to be a coincidental result of two different dynamic behaviors. The plate's transient off-axis radiation (e.g. 100 mm) appears to be dispersive, and is undoubtedly not piston like.

4.2. Second hypothesis: dispersed acoustic wave

It can be shown that except for the impacted area itself, a time delay occurs in the forced response of the plate (in the course of contact). In fact, elastic waves start propagating in the plate as soon as the contact force is initiated. Fig. 7 illustrates such propagation. Transverse displacements of the plate were calculated using by Eq. (4), for points located along the plate horizontal centerline. Point locations vary from -300 to $+300$ mm, measured from the impact point as shown in Fig. 7a. Several curves are plotted at time increments of 0.03 ms when the force is applied. From Fig. 7b, an increasing transverse displacement of the impact point (position 0 mm) is observed while the plate is subjected to the impact force (from 0 to 0.15 ms). Meanwhile, the radius of the deformed area of the plate increases regularly. One can clearly see, for instance, that points located at ± 50 mm are still at rest at time 0.03 ms, and are in motion at time 0.06 ms. Similarly, points located at ± 100 mm are still at rest at time 0.06 ms, and are in motion at time 0.09 ms, and so on. Because all points are not accelerated synchronously, the initial transient noise of the plate differs from the acceleration noise of a piston, for a same force excitation.

Although the impact force was applied at a single point on the plate, there is no clear boundary between what would be considered to be the "forced" or "initial deformation" and the "bending wave radiation".

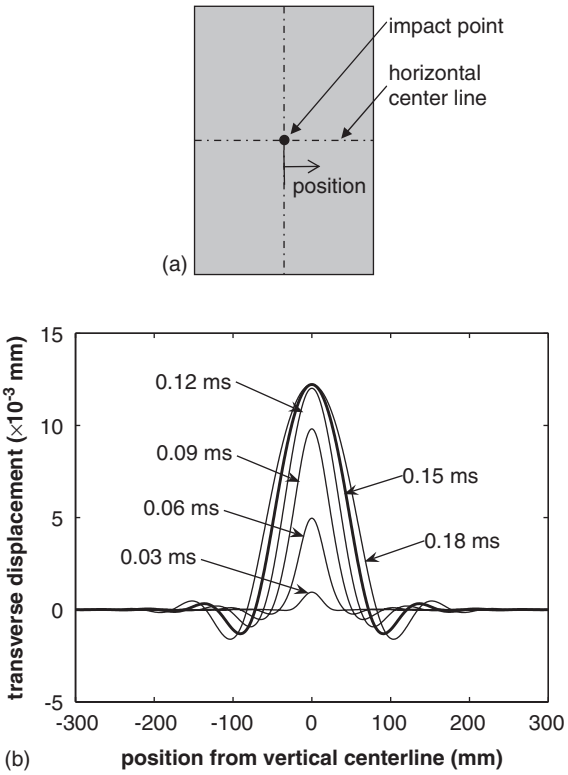

Fig. 7. Transverse displacement of plate along horizontal centerline, calculated from Eq. (4): (a) plate configuration, and (b) displacement at various times in the course of impact.

Indeed, dispersion ripples can be seen near the edge of the deformed area of the plate (Fig. 7). Ripples occur while the force is still active (<0.15 ms) and while the impact point is still being pushed away from its initial position. These ripples propagate the higher-frequency components of the bending wave, while lower frequency components are still in the central part of the deformed area of the plate.

Along the surface of the plate ($\theta = 90^\circ$), velocity continuity forces the initial transient noise to follow the dispersive bending wave in the plate, for all frequencies above the critical frequency. The supercritical frequencies of the bending wave travel faster than airborne sound waves. Therefore, with reference to Eq. (8), the earliest air pressure variations on the plate, at a distance (R) from the impact axis are caused by the passage of the bending wave at this position, even though acoustic pressures were created by earlier deformations of the plate, closer to the impact point. Consequently, the initial part of surface acoustic waves must travel at the same velocity as the bending wave in the plate.

At any given frequency, the acoustic wavefront in the fluid medium around the plate (i.e. air in the present case) travels at sound velocity c. The sound speed c is "measured" perpendicular to the wavefront. This is true for all sounds, including initial transient noises from impacted plates. Fig. 8 illustrates the propagation of a few supercritical frequency components of the initial transient noise. The plate, shown as a thick line, is impacted at its center. Acoustic radiation is shown on one side of the plate only. Along the plate, the supercritical components travel at the same supersonic velocity as the bending wave ($c_b \propto \omega^{1/2}$), as mentioned above. High-frequency components travel faster than lower-frequency components in this plane. Normal to the acoustic wavefronts, the velocity is c. Because c_b and c have two different values, the wavefronts are oblique, due to pressure continuity in the medium [4].

In addition, because c_b is higher for upper frequency components, and c is constant for all frequencies, the propagation angle (α) is different for each supercritical component. In Fig. 8, the sound speed at high frequencies ($c_h = c$) and at lower frequencies $c_\ell = c$ are oriented normal to their respective wavefront. Both have the same value, but they have different angles (α) with respect to the impact axis. Therefore, the propagation angle from the impact axis is greater for lower frequency components than it is for upper frequency components [10]. Wåhlin et al. have obtained clear experimental images of these various propagation angles, using an interferometry technique on a real impacted plate [4]. The propagation angle is obtained through the geometric relationship [4]:

$$\sin(\alpha) = \frac{c}{c_b}. \tag{13}$$

Considering the above, it is noticeable that for near field observation points located at relatively large angles θ from the impact axis (as in Fig. 8), supercritical noise components will reach the point at different times. Simple geometry gives the apparent wavefront velocity of one frequency component at angle θ:

$$c_\theta = \frac{c}{\cos(\theta - \alpha)} \quad \text{for} \quad \alpha \leqslant \theta \leqslant \pi/2. \tag{14}$$

Obviously, the apparent velocity is equal to the sound speed in air ($c_\theta = c$) when $\theta = \alpha$, and to the bending wave velocity ($c_\theta = c_b$) when $\theta = \pi/2$. At small observation angles ($\theta < \alpha$), the wave velocity is c for all

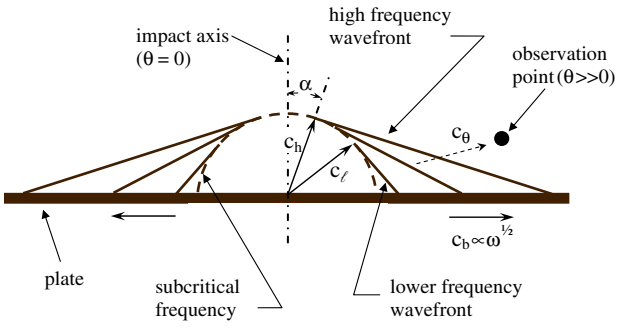

Fig. 8. Propagation of the initial transient noise by means of a dispersive wave.

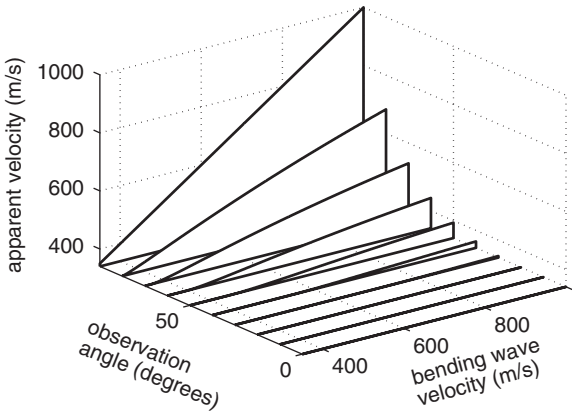

Fig. 9. Apparent velocity of supercritical noise components at various observation angles from impact axis.

frequencies. Apparent velocities were calculated using Eqs. (13) and (14), and are plotted in Fig. 9 for various observation angles from 0 to $\pi/2$. In this figure, bending wave velocities vary from $c_b = c = 340\,\mathrm{m/s}$ to $c_b = 1000\,\mathrm{m/s}$, thereby covering a frequency range of 22 kHz. This plot highlights the fact that for a given frequency (or bending wave velocity), the apparent velocity increases with the observation angle. More importantly, the figure clearly shows that for a given observation angle, the apparent velocity increases with the bending wave velocity (or frequency).

Therefore, the supercritical part of the initial transient noise of an impacted plate is being dispersed, due to velocity continuity with the plate, and to pressure continuity in the propagating medium. From Fig. 9, the effects of dispersion seem to be negligible at small observation angles ($\theta \leqslant 20^\circ$), but become much greater at large observation angles. As a result, dispersion of the initial transient noise may account for the appearance of early acoustic pressure oscillations in the vicinity of an impacted plate.

4.3. Analytical models and comparison

Two propagation models were created, and simulations were performed on a numeric test signal that corresponds to the above configuration A (low energy). The test signal represents the initial transient noise as a function of time, at 50 mm along the impact axis. This position is referred to as the "acquisition" point. The test signal is easily obtained from the previous model (using Eq. (1)), and is shown as a dotted line in the various frames of Fig. 10. After the end of contact ($t > \tau'$), all pressure values are gradually forced to zero, in order to eliminate the following ringing signal.

Each model represents one of the hypothetical means of propagation described above, for the initial transient noise: a piston-like, non-dispersive radiation, or a dispersed acoustic wave. The positions where the acoustic pressure signal is reconstructed are referred to as the simulation points. They are located at 50 mm from the surface of the plate, and at observation angle $\theta = 23^\circ$, 52°, 64°, and 71°. In the non-dispersive, spherical wave model, the test signal is subjected both to the time delay and amplitude decay that correspond to the additional traveling distance with respect to the acquisition point.

In the dispersive model, sub-critical frequencies of the test signal are treated in the same way as in the non-dispersive model. However, the supercritical frequencies are subjected to a mathematical transformation that involves phase shifts. As was seen in Fig. 8, the propagation angle α is smaller for higher frequencies. For a given observation point $P(r, \theta)$, distances (d_ω) traveled by each frequency component of the acoustic wave are calculated based on the geometrical considerations in Eq. (13). The corresponding phase shifts [$\exp(-j\xi_\omega)$] are applied to the test signal:

$$\xi_\omega = \frac{\omega \mathrm{d}_\omega}{c_p}. \tag{15}$$

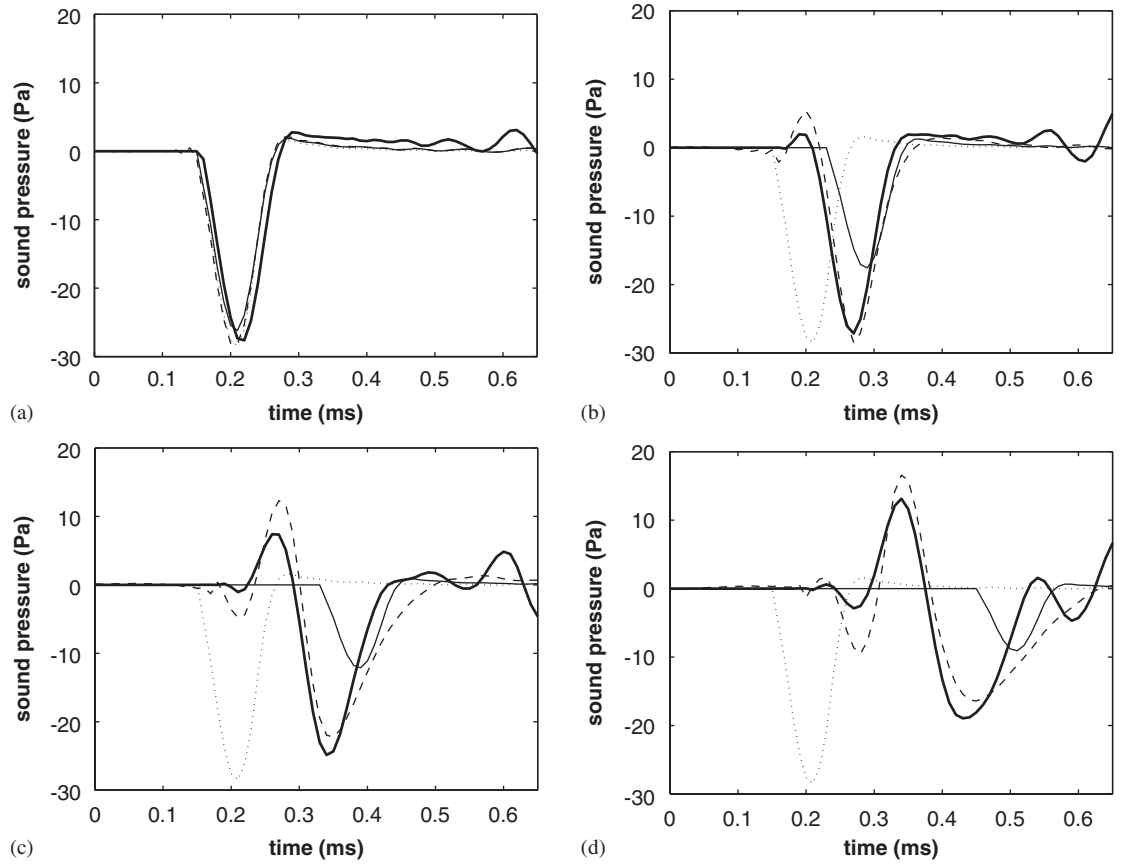

Fig. 10. Comparison of the dispersive (- - -) and non-dispersive (——) propagation models for the initial transient noise from the test signal (· · ·). The initial transient acoustic wave (——) was calculated using Eq. (11). Observation angle θ is 23° in frame (a), 52° in frame (b), 64° in frame (c) and 71° in frame (d).

The bending wave velocity c_b is given as a function of ω, the radial frequency [11]:

$$c_b = \sqrt[4]{\frac{E_p h \omega^2}{12\rho_p(1-v_p^2)}}. \tag{16}$$

In Fig. 10 are shown the simulation results from the two models. The thick solid line is the complete impact noise, computed from Eq. (11) (equivalent to the experimental data). It serves as the reference sound. The thin solid line and the dashed line represent the non-dispersive and the dispersive models, respectively. The simulations are quite conclusive. When the in-axis initial transient noise test signal is propagated away from the impact axis as a piston-like, non-dispersive airwave (thin solid line), the reconstructed signal has no affinity whatsoever with the reference sound. The amplitude of the reconstructed signal is much smaller than the reference sound, and the time delay is excessive. Superimposition of a gradually developing ringing noise would not suffice to generate the reference sound. In contrast, when the test signal is propagated through the dispersive model (dashed line), it is very similar to the reference sound. Both amplitude and time delay are reasonably close to that observed in the reference sound. As expected, an initial positive peak develops as the simulation point P moves away from the impact axis, and additional peaks arise. The initial part of the reference sound is well represented by the reconstructed signal. The later part of the simulated signals diverge from the reference sound because the test signal does not include ringing (seen as developing oscillations in the reference sound, starting around $t = 0.5$ ms).

5. Conclusion

The purpose of this study was to demonstrate that the initial transient noise from an impacted plate is partially structure-borne. Near field sound radiation from a theoretical solution was compared with experimental data. Two different partial solutions were compared to the complete solution. The results show that the initial transient noise is structure-borne. It is dispersive and the acoustic trace on the plate matches the supersonic bending wave components within the plate. Close to the impact axis ($0^\circ \leqslant \theta \leqslant 20^\circ$), acoustic dispersion appears negligible. Effects of dispersion increase with the observation angle. Along the impact axis, the initial transient noise and the impact force present similar time signals, both in shape and duration. At low impact energy, the shaped is a short half-sine, whereas high-energy impacts yield a longer, exponentially decreasing shape. For a large plate and short contact duration, the initial transient noise and ringing noise may be considered sequential; otherwise, there is an overlap. It was also verified that the initial transverse acceleration and the initial transient noise from a central impact on a rectangular plate are symmetrical about the impact axis.

Acknowledgments

This work was supported by the Natural Sciences and Engineering Research Council of Canada.

References

[1] A. Akay, A review of impact noise, *Journal of the Acoustical Society of America* 64 (4) (1978) 977–978.
[2] E.J. Richards, M.E. Westcott, R.K. Jeyapalan, On the prediction of impact noise I: acceleration noise, *Journal of Sound and Vibration* 62 (1979) 547–575.
[3] L.A. Wood, K.P. Byrne, Acceleration noise generated by a random repeated impact process, *Journal of Sound and Vibration* 88 (1983) 489–499.
[4] A.O. Wåhlin, P.O. Gren, N.-E. Molin, On structure-borne sound: experiments showing the initial transient acoustic wave field generated by an impacted plate, *Journal of the Acoustical Society of America* 96 (5) (1994) 2791–2796.
[5] A. Akay, M. Latcha, Sound radiation from an impact-excited clamped circular plate in an infinite baffle, *Journal of the Acoustical Society of America* 74 (2) (1983) 640–648.
[6] W. Heitkämper, Näherungsweise Berechnung der Schallabstrahlung von storßartig angeregten Platten, *Acustica* 58 (3) (1985) 141–148.
[7] W. Goldsmith, *Impact*, Edward Arnold Ltd., USA, 1960.
[8] M.J. Crocker, *Handbook of Acoustics*, Wiley, USA, 1998.
[9] A. Ross, G. Ostiguy, M. Amram, Properties of the transient acoustic field of an impacted plate, *Proceedings of the Ninth International Congress on Sound and Vibration,* University of Central Florida, Orlando, FL, 2002.
[10] D. Takahashi, Frequency analysis of sound radiation from an impact-excited plate, *Journal of the Acoustical Society of America* 91 (5) (1991) 2708–2713.
[11] F. Fahy, *Sound and Structural Vibration: Radiation, Transmission and Response*, Academic Press Inc., London, 1985.